A new approach for obtaining sequential assignment of large proteins

Perttu Permi[a],* & Arto Annila[b]

[a]*Institute of Biotechnology, NMR Laboratory, P.O. Box 56, FIN-00014, University of Helsinki, Helsinki, Finland*
[b]*VTT Biotechnology, FIN-02044 VTT, Espoo, Finland*

Abstract

A novel NMR experiment for obtaining sequential assignment of large proteins and protein complexes is described. The proposed method takes full advantage of transverse relaxation optimized spectroscopy (TROSY) and utilizes spin-state-selection to distinguish between intraresidual and sequential connectivities in the HNCA-TROSY-type correlation experiment. Thus, the intra- and interresidual cross peaks can be identified without relaying magnetization via carbonyl carbon, which relaxes very rapidly at the high magnetic fields where TROSY is most efficient. In addition, the presented method enables measurement of several scalar and residual dipolar couplings, which can potentially be used for structure determination of large proteins.

Introduction

Chemical shift assignment of NMR resonances to individual atoms forms a substratum for any structural study by high resolution NMR spectroscopy. Assignment of ^{15}N, ^{13}C labeled protein samples is usually derived from a pair of HN detected three-dimensional experiments i.e. (CT)-HNCA and (CT)-HN(CO)CA (or alternatively HNCACB and HN(CO)CACB), to connect both intraresidual and sequential ^{13}C$^{\alpha}$ (or ^{13}C$^{\beta}$) resonances with intraresidual ^{15}N and ^{1}H^{N} resonances (Yamazaki et al., 1994a,b; Shan et al., 1996). The (CT)-HN(CO)CA experiment is necessary to ensure unambiguous assignment of intra- and interresidual ^{15}N, ^{13}C$^{\alpha}$ connectivities, since it is not always clear from the peak intensity which one of the cross peaks belongs to ^{13}C$^{\alpha}(i)$ and ^{13}C$^{\alpha}(i-1)$ due to comparable sizes of $^{1}J_{NC\alpha}$ and $^{2}J_{NC\alpha}$ couplings. Furthermore, assignment of larger proteins (300–400 residues) necessitates perdeuteration, i.e., substituting aliphatic protons for deuterons, in order to decelerate ^{13}C$^{\alpha}$ as well as ^{1}H^{N} relaxation (Gardner and Kay, 1997).

Application of transverse relaxation optimized spectroscopy (TROSY) (Pervushin et al., 1997) has further pushed the molecular size-limit over 100 kDa when using highly perdeuterated proteins or protein complexes (Salzmann et al., 2000). The TROSY spectroscopy works best at high magnetic fields (∼1 GHz) where cancellation of dipolar and chemical shift anisotropy (CSA) relaxation mechanisms for ^{15}N and ^{1}H^{N} spins is optimal (Pervushin et al., 1997). However, carbonyl carbon has large CSA and consequently the transverse relaxation rate of ^{13}C$'$ increases very rapidly with increasing magnetic field. The ^{13}C$'$ transverse relaxation rate has a quadratic dependence on the magnetic field strength and is also proportional to the molecule's rotational correlation time. Therefore NMR experiments utilizing the ^{13}C$'$ spin are best carried out at field strengths smaller than 600 MHz proton frequency, far from the optimum for the TROSY effect. It has been shown that for a 110 kDa protein the rapid ^{13}C$'$ relaxation deteriorates the HN(CO)CA experiment compared to HNCA already at 500 MHz (Salzmann et al., 2000). For this reason, it would be desirable for large systems if sequential assignment could be obtained without relaying coherence via carbonyl carbon.

In this paper we show that spin-state-selective filtering can be employed to distinguish the intra- and interresidual connectivities without using the

*To whom correspondence should be addressed. E-mail: Perttu.Permi@helsinki.fi
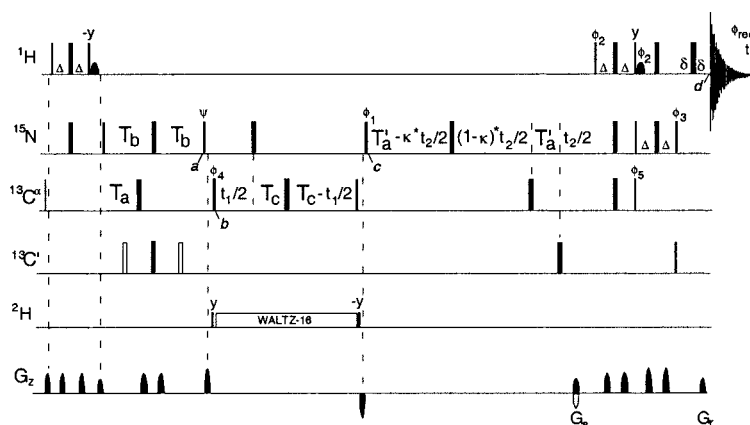
Figure 1. Pulse scheme of the multipurpose CT-HNCA (MP-CT-HNCA) experiment. Narrow and wide bars correspond to 90° and 180° flip angles, respectively, applied with phase x unless otherwise indicated. All rectangular $^{13}C'$ and $^{13}C^\alpha$ 90° (180°) pulses were applied with a strength of $\Omega/\sqrt{15}$ ($\Omega/\sqrt{3}$), where Ω is the frequency difference between the centers of the $^{13}C'$ and $^{13}C^\alpha$ regions. All $^{13}C^\alpha$ pulses were applied on-resonance and $^{13}C'$ pulses off-resonance with phase modulation by Ω. The ^1H, ^{15}N, $^{13}C'$ and $^{13}C^\alpha$ carrier positions are 4.7 (water), 120 (center of ^{15}N spectral region), 176 (center of $^{13}C'$ spectral region), and 56 ppm (center of alpha carbon region), respectively. Frequency discrimination in F_2 was obtained using the sensitivity and gradient enhanced TROSY scheme, i.e. by collecting two data sets, (I): $\phi_2 = x$; $\phi_3 = y$, (II): $\phi_2 = -x$; $\phi_3 = -y$ simultaneously changing the gradient polarity (Weigelt, 1998). Alternatively, several other, but slightly different, SE-TROSY schemes can be used as well (Andersson et al., 1998b; Meissner et al., 1998b; Pervushin et al., 1998; Rance et al., 1999; Yang and Kay, 1999). Quadrature detection in the $^{13}C^\alpha$ dimension was obtained by States-TPPI (Marion et al., 1989) applied to ϕ_4. Pulsed field gradients were inserted as indicated for coherence transfer pathway selection and residual water suppression. Deuterium is decoupled using the WALTZ-16 sequence (Shaka et al., 1983). In order to differentiate intraresidual from sequential connectivities, the in- and antiphase data were recorded in an interleaved manner and subsequently added and subtracted to separate the multiplet components to two subspectra. Delay durations: $\Delta = 1/(4J_{HN})$; $T_a = 12-14$ ms; $T'_a = T_a - \Delta$; $T_b = 1/(4J_{NC'})$; δ = gradient + field recovery delay; $T_c = 1/(8J_{C^\alpha C^\beta})$ or $1/(2J_{C^\alpha C^\beta})$ depending on the relaxation rate of $^{13}C^\alpha$; $0 \le \kappa \le T'_a/t_{2,max}$. Gradient strengths (durations): $G_s = 30$ G/cm (1.25 ms), $G_r = 29.6$ G/cm (0.125 ms). The water signal was suppressed by a water flip-back technique to ensure that most of the water magnetization was preserved along the z-axis throughout the pulse sequences and residual transverse magnetization was effectively dephased by the pulsed field gradients (Grzesiek and Bax, 1993). The phase cycling scheme for the in-phase spectrum is $\phi_1 = y$; $\phi_2 = x$; $\phi_3 = x$; $\phi_4 = x, -x$; $\phi_5 = 2(x), 2(-x)$; $\phi_{rec.} = x, -x$; $\psi = y$. For the antiphase spectrum, ψ is incremented by 90°. The last 90°($^{13}C^\alpha$) pulse removes the dispersive contribution from the lineshape (Permi et al., 1999a). The last 90° pulse on $^{13}C'$ (optional) removes the E.COSY pattern if desired.

HN(CO)CA experiment. Previously spin-state-selective filtering has been applied to remove unnecessary spectral crowding due to coupled evolution (Meissner et al., 1997, 1998a; Andersson et al., 1998a; Ottiger et al., 1998; Permi et al., 1999a,b). In addition, we have shown that the spin-state-selective filtering can be used in a way to mimick selective decoupling in order to simplify multiplet substructure (Permi and Annila, 2000). Now we demonstrate that the intra- and interresidual correlations can be identified by editing the spin-state of the sequential $^{13}C'$ spin.

Experimental

The in- and antiphase MP-CT-HNCA-TROSY data sets were recorded from U-^{15}N, ^{13}C, ^{2}H-enriched 30.4 kDa E2 endocellulase (286 amino acid residues) from *Thermomonospora fusca* (Spezio et al., 1993) at 5 °C on a Varian UNITY INOVA 800 NMR spectrometer using 16 transients per FID. In the t_1, t_2

and t_3 dimensions 34, 39, 512 complex points were recorded respectively, with corresponding acquisition times of 6.9 ms, 14.5 ms and 43 ms. Total acquisition time was 68 h. The data were zero-filled to $512 \times 128 \times 1024$ points before Fourier transform and phase-shifted squared sine-bell window functions were applied in all dimensions. The corresponding HN(CO)CA experiment was recorded and processed with similar parameters. Total acquisition time for the HN(CO)CA experiment was 34 h.

The in- and antiphase MP-CT-HNCA-TROSY spectra using a constant-time delay of 28 ms were recorded from U-^{15}N, ^{13}C, ^{2}H-enriched E2 at 40 °C on a Varian UNITY INOVA 600 NMR spectrometer using 8 scans per FID. Acquisition times of 27.8, 14.5 and 56 ms were used in t_1, t_2, and t_3, respectively, corresponding to 100, 28, 512 complex points. The data were zero-filled to $512 \times 128 \times 1024$ points before Fourier transform and phase-shifted squared sine-bell window functions were applied in all dimensions.

Theory

We describe a multipurpose HNCA (MP-CT-HNCA-TROSY) experiment, largely similar to the familiar CT-HNCA experiment, to correlate $^1H^N(i)$, $^{15}N(i)$, $^{13}C^\alpha(i)/(i-1)$ spins in large proteins (Figure 1). The flow of coherence in this novel experiment is only explained on its essential parts.

In the MP-CT-HNCA experiment the spin-state-selective filter matched to the $^1J_{NC'}$ coupling (Permi et al., 1999b) is utilized during the magnetization transfer step from the ^{15}N to the $^{13}C^\alpha$ spin. The $^1H^N$ magnetization is initially transferred to the directly bound ^{15}N spin. During the following delay $2T_b$, the magnetization is transferred to the interresidual $^{13}C'$ spin in one experiment referred to here as the antiphase experiment. In addition, evolution of the $^1J_{NC^\alpha}$ and $^2J_{NC^\alpha}$ couplings during the delay $2T_a$ dephase the ^{15}N coherence with respect to the $^{13}C^\alpha(i)$ or $^{13}C^\alpha(i-1)$ spin. A similar magnetization transfer pathway, although for different purposes, has been used by others (Szyperski et al., 1995; Meissner et al., 1998a; Astrof et al., 1998; Konrat et al., 1999). Thus, the desired magnetization at time point a can be described by the density operators $H_z^N(i)N_y(i)C_z'(i\text{-}1)C_z^\alpha(i)$ and $H_z^N(i)N_y(i)C_z'(i\text{-}1)C_z^\alpha(i-1)$ for the intra- and interresidual correlation, respectively. Subsequently, the magnetization is transferred to $H_z^N(i)N_z(i)C_z'(i-1)C_y^\alpha(i)$ and $H_z^N(i)N_z(i)C_z'(i-1)C_y^\alpha(i-1)$ coherences (time point b) followed by a constant-time evolution period. During this period, the $^{13}C^\alpha$ chemical shift is labeled, and concomitantly evolution of the ^1J and ^2J couplings to $^{13}C'$ spins within the same and sequential residue occurs. The ^{15}N chemical shift frequencies are labeled during the semi-constant time TROSY evolution period (Permi and Annila, 2000), and finally the desired magnetization is transferred back to the amide proton using a sensitivity enhanced gradient selected TROSY scheme (Weigelt, 1998), which provides good water suppression enabling use of larger receiver gain, essential for insensitive experiments. The detectable magnetization components in the antiphase experiment prior to the acquisition period (time point d) for the intra- $C^\alpha(i)$ and interresidual $C^\alpha(i-1)$ connectivities, respectively, are:

$$\{H_y^N(i)C_z'(i-1)\cos(\pi^2 J_{C^\alpha(i)C'(i-1)}t_1)$$
$$\cos(\pi^1 J_{C^\alpha(i)C'(i)}t_1) + H_y^N(i)C_z'(i)$$
$$\sin(\pi^2 J_{C^\alpha(i)C'(i-1)}t_1)\sin(\pi^1 J_{C^\alpha(i)C'(i)}t_1)\}$$
$$\cos(\omega_{C^\alpha(i)}t_1) + \{H_y^N(i)\sin(\pi^2 J_{C^\alpha(i)C'(i-1)}t_1)$$
$$\cos(\pi^1 J_{C^\alpha(i)C'(i)}t_1) + H_y^N(i)C_z'(i-1)C_z'(i)$$
$$\cos(\pi^2 J_{C^\alpha(i)C'(i-1)}t_1)\sin(\pi^1 J_{C^\alpha(i)C'(i)}t_1)\}$$
$$\sin(\omega_{C^\alpha(i)}t_1)$$

and

$$\{H_y^N(i)C_z'(i-1)\cos(\pi^1 J_{C^\alpha(i-1)C'(i-1)}t_1)$$
$$\cos(\pi^2 J_{C^\alpha(i-1)C'(i)}t_1) + H_y^N(i)C_z'(i)$$
$$\sin(\pi^1 J_{C^\alpha(i-1)C'(i-1)}t_1)\sin(\pi^2 J_{C^\alpha(i-1)C'(i)}t_1)\}$$
$$\cos(\omega_{C^\alpha(i-1)}t_1) + \{H_y^N(i)\sin(\pi^1 J_{C^\alpha(i-1)C'(i-1)}t_1)$$
$$\cos(\pi^2 J_{C^\alpha(i-1)C'(i)}t_1) + H_y^N(i)C_z'(i-1)C_z'(i)$$
$$\cos(\pi^1 J_{C^\alpha(i-1)C'(i-1)}t_1)\sin(\pi^2 J_{C^\alpha(i-1)C'(i)}t_1)\}$$
$$\sin(\omega_{C^\alpha(i-1)}t_1).$$

The intra- and interresidual cross peaks are distinguished from each other by recording another experiment, referred to here as the in-phase experiment, in which dephasing of the ^{15}N coherence due to the $^1J_{NC'}$ coupling during the delay $2T_b$ is removed by applying two $180°(^{13}C')$ pulses during $2T_b$, as illustrated by unfilled wide bars in Figure 1. Thus, the desired magnetization components prior to acquisition, analogously for the antiphase experiment, at the time point d are:

$$\{H_y^N(i)\cos(\pi^2 J_{C^\alpha(i)C'(i-1)}t_1)\cos(\pi^1 J_{C^\alpha(i)C'(i)}t_1)$$
$$+ H_y^N(i)C_z'(i-1)C_z'(i)\sin(\pi^2 J_{C^\alpha(i)C'(i-1)}t_1)$$
$$\sin(\pi^1 J_{C^\alpha(i)C'(i)}t_1)\}\cos(\omega_{C^\alpha(i)}t_1)+$$
$$\{H_y^N(i)C_z'(i-1)\sin(\pi^2 J_{C^\alpha(i)C'(i-1)}t_1)$$
$$\cos(\pi^1 J_{C^\alpha(i)C'(i)}t_1) + H_y^N(i)C_z'(i)$$
$$\cos(\pi^2 J_{C^\alpha(i)C'(i-1)}t_1)\sin(\pi^1 J_{C^\alpha(i)C'(i)}t_1)\}$$
$$\sin(\omega_{C^\alpha(i)}t_1)$$

and

$$\{H_y^N(i)\cos(\pi^1 J_{C^\alpha(i-1)C'(i-1)}t_1)$$
$$\cos(\pi^2 J_{C^\alpha(i-1)C'(i)}t_1) + H_y^N(i)C_z'(i-1)C_z'(i)$$
$$\sin(\pi^1 J_{C^\alpha(i-1)C'(i-1)}t_1)\sin(\pi^2 J_{C^\alpha(i-1)C'(i)}t_1)\}$$
$$\cos(\omega_{C^\alpha(i-1)}t_1) + \{H_y^N(i)C_z'(i-1)$$
$$\sin(\pi^1 J_{C^\alpha(i-1)C'(i-1)}t_1)\cos(\pi^2 J_{C^\alpha(i-1)C'(i)}t_1)+$$
$$H_y^N(i)C_z'(i)\cos(\pi^1 J_{C^\alpha(i-1)C'(i-1)}t_1)$$
$$\sin(\pi^2 J_{C\alpha(i-1)C'(i)}t_1)\}\sin(\omega_{C^\alpha(i-1)}t_1).$$

Now, by adding the corresponding antiphase and in-phase data sets two subspectra result where intraresidual cross peaks appear at $\omega_{C^\alpha(i)} \pm \pi^1 J_{C'C^\alpha}$, $\omega_{N(i)} - \pi^1 J_{NH}$, $\omega_{H^N(i)} + \pi^1 J_{NH} \pm \pi^3 J_{H^NC'}$, and $\omega_{C^\alpha(i)} \pm \pi^1 J_{C'C^\alpha}$, $\omega_{N(i)} - \pi^1 J_{NH}$, $\omega_{H^N(i)} + \pi^1 J_{NH} \pm \pi^3 J_{H^NC'}$, and sequential connectivities at $\omega_{C^\alpha(i-1)} +$
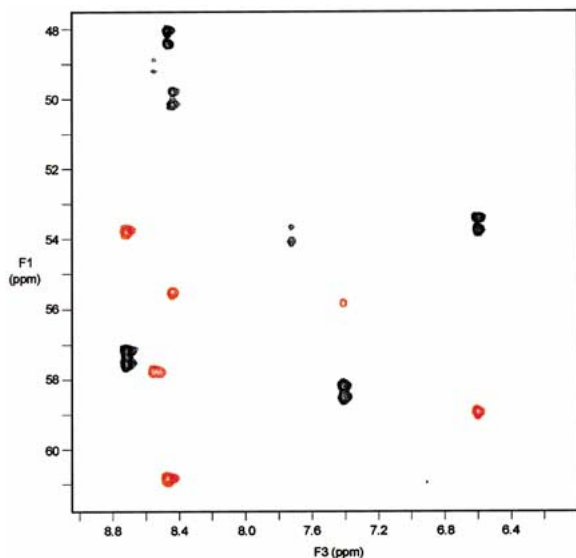
Figure 2. One subspectrum of the MP-CT-HNCA-TROSY experiment from E2 at 40 °C showing intra- and interresidual correlations as doublets and singlets (red contours), respectively. The constant-time delay (2T$_C$) was in this case set to 28 ms.

$\pi^1 J_{C'C^\alpha}$, $\omega_{N(i)} - \pi^1 J_{NH}$, $\omega_{H^N(i)} + \pi^1 J_{NH} - \pi^2 J_{H^N C'}$, and $\omega_{C^\alpha(i-1)} - \pi^1 J_{C'C^\alpha}$, $\omega_{N(i)} - \pi^1 J_{NH}$, $\omega_{H^N(i)} + \pi^1 J_{NH} + \pi^2 J_{H^N C'}$. The intra- and interresidual cross peaks can be discerned from the multiplet structure in the subspectra. Interresidual resonances appear as singlets in both subspectra displaced by ∼55 Hz $^1 J_{C^\alpha(i-1)C'(i-1)}$ coupling whereas intraresidual cross peaks appear as doublets separated by $^1 J_{C^\alpha(i)C'(i)}$ coupling (Figure 2). In fact, also the intraresidual cross peak is shifted in the F$_1$-dimension by the $^2 J_{C^\alpha(i)C'(i-1)}$ coupling between two subspectra but in practice this coupling is at least one order of magnitude smaller than $^1 J_{C^\alpha C'}$. Therefore, even if the resolution in the F$_1$-dimension prevents separation of the $^1 J_{C^\alpha(i)C'(i)}$ coupling, the inter- and intraresidue cross peaks can be easily differentiated by the peak picking routines. A more thorough inspection of the resulting density operators reveals that the MP-CT-HNCA experiment allows measurement of several couplings. Measurement and analysis of the couplings is beyond the scope of this paper. If desired, the emerging E.COSY patterns can be removed by applying a 90°(^{13}C′) purge pulse prior to acquisition (Figure 1).

Results and discussion

To compare the proposed approach with the pair of CT-HNCA and CT-HN(CO)CA experiments, the effects of protein size and applied magnetic field strength on the transverse relaxation time of ^{13}C′ have to be considered in detail. The transverse relaxation time for the ^{13}C′ spin in the protein main chain, by excluding flexible regions, can be approximated by Equation 1 (Hu and Bax, 1997):

$$T_{2C'} \sim 1/[\tau_c(3/4 + B^2/150)] \tag{1}$$

where τ_c (ns) is the correlation time of the molecule, and B (T) is the strength of the magnetic field (Figure 3). For example, for a 80 kDa system with $\tau_c = 35$ ns at 500 MHz, the $T_{2C'}$ is close to 18 ms. At the field strength of 900 MHz, presently the highest field available, $T_{2C'}$ is on the order of 7 ms. In the latter case, the sensitivity loss during C′ to C$^\alpha$ out-and-back-transfer steps can be nearly 10-fold, leading to higher sensitivity of the sequential correlation in the MP-CT-HNCA experiment. Hence, the coherence transfer efficiency of the experiments relaying magnetization through ^{13}C′ drops dramatically compared to the HNCA-type experiments with increasing protein size and magnetic field strength. Palmer and co-workers have estimated that for large proteins at 900 MHz, the intensity of interresidue correlation available from HN(CO)CA becomes smaller than the intensity of sequential correlation in the HNCA-type experiment (Loria et al., 1999).

It is noteworthy that in the MP-CT-HNCA experiment, if $t_{1,max}$ is shorter or on the order of 9 ms ($\geq 1/(2J_{C'C^\alpha})$), the sensitivity of the in-phase experiment is $\sqrt{2}$ times higher than in the subspectra. This can be easily realized by comparing the in-phase experiment with long $t_{1,max}$ to the in-phase experiment with short $t_{1,max}$. The latter can be understood as the usual CT-HNCA experiment (due to unresolved $^1 J_{C^\alpha C'}$ coupling i.e. α and β spin-states are superimposed), and therefore its sensitivity is approximately two times higher (within the same experimental time). Now, if the antiphase data set is added to, or subtracted from, the in-phase experiment with long $t_{1,max}$, one of the spin-states is cancelled whereas the other one is reinforced. However, the overall sensitivity of the resulting subspectra is only $\sqrt{2}$ higher due to increased noise. The same holds also for the in-phase experiment with short $t_{1,max}$ except that one of the superimposing spectral lines, corresponding to the α- or β-spin-state, is now removed and virtually replaced
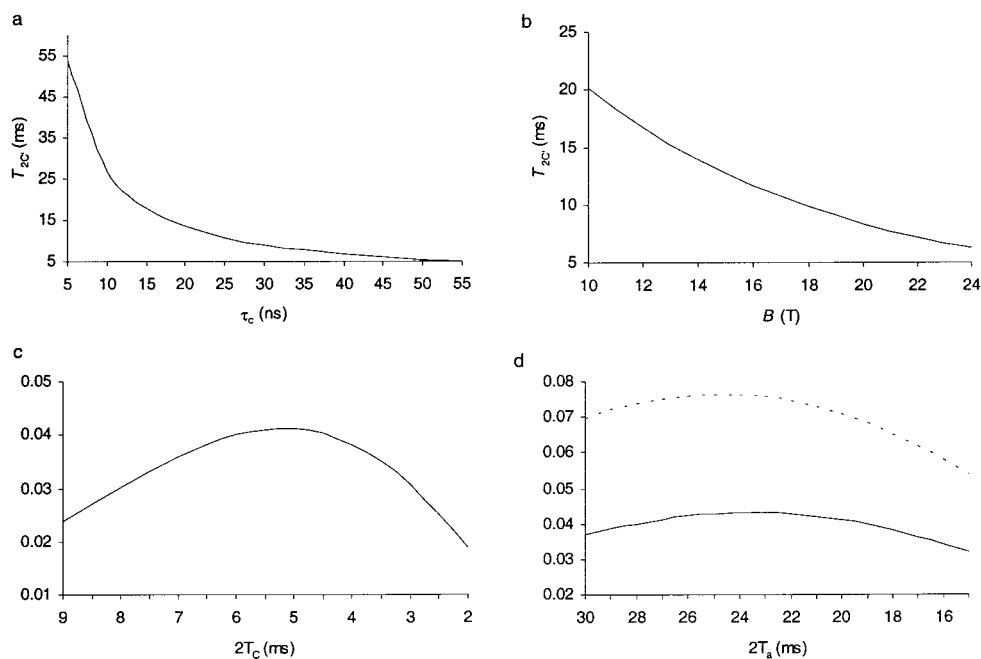
Figure 3. Carbonyl carbon ($^{13}C'$) transverse relaxation time as a function of protein rotational correlation time τ_c (a) and applied magnetic field strength (b). The equation $T_{2C'} = 1/[\tau_c(0.75+B^2/150)]$ (Hu and Bax, 1997) is plotted with the following parameters (a) $B = 21.1$ T and (b) $\tau_c = 35$ ns. Coherence transfer efficiencies as a function of $2T_c$ for the CT-HN(CO)CA (c) and as a function of $2T_a$ for the MP-CT-HNCA (d) experiments. The transfer functions were calculated according to Equations 2 and 3, respectively, using the following parameters: $T_{2N} = 50$ ms, $T_{2C'} = 7$ ms, $2T_N = 26$ ms, $2T_b = 33$ ms, $^1J_{NC'} = 15$ Hz, $^1J_{NC\alpha} = 10$ Hz (9 Hz for dashed line), $^2J_{NC\alpha} = 7$ Hz (9 Hz for dashed line), $^1J_{C'C\alpha} = 53$ Hz.
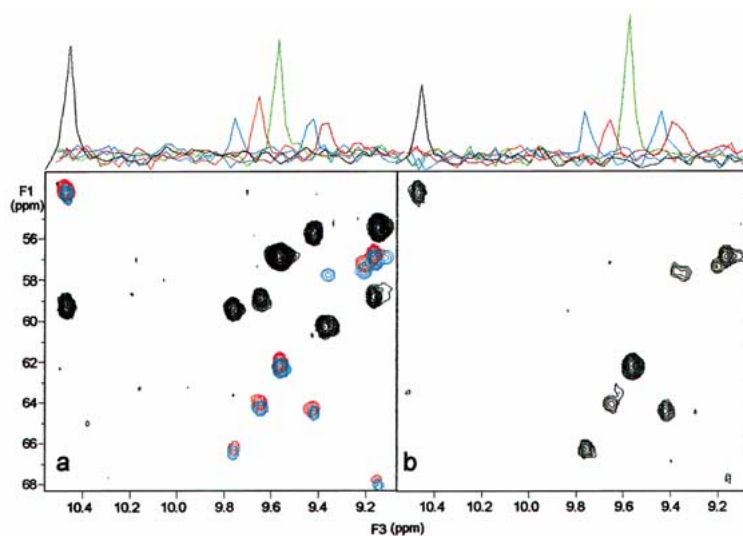

Figure 4. Selected 2D planes of the MP-CT-HNCA (a) and CT-HN(CO)CA (b) experiments. Two MP-CT-HNCA-TROSY subspectra are shown overlaid, with α and β states of the interresidual correlations in red and blue contours, respectively. Displacement of up- and downfield components of the interresidual cross peak between two subspectra is ∼ 50–55 Hz, enabling identification of sequential connectivities. The corresponding intraresidual correlations are separated by small $^2J_{C\alpha C'}$ and the two subspectra are practically superimposed. Intraresidual and sequential connectivities can be easily distinguished even if the $^1J_{C\alpha C'}$ coupling is not resolved. The cross peak displacement between two subspectra in the F$_3$-dimension is due to small $^2J_{HN(i)C'(i-1)}$ coupling and can be easily removed by the purge pulse. The corresponding cross-sections are shown for some interresidual connectivities to document sensitivity between the MP-CT-HNCA (a) and CT-HN(CO)CA (b) experiments. The cross-sections, in the case of the MP-CT-HNCA experiment, are taken from the 'in-phase' spectrum, which has $\sqrt{2}$ times higher sensitivity than the two subspectra as described in the text.

by the spectral line corresponding to the α- or β-spin-state in the antiphase data set. Thus, the net product of this addition, or subtraction, is increased noise by a factor of $\sqrt{2}$. For this reason, when the constant-time delay is 7 ms for instance, it is advantageous to use the in-phase experiment exclusively to identify very weak interresidual cross peaks in the first place. The weakest signals usually arise from residues where $^1J_{NC^\alpha}$ is large and $^2J_{NC^\alpha}$ is small (*vide infra*), i.e., the intensity of the sequential correlation is significantly smaller than that of the intraresidual correlation. If the inter- and intraresidual correlations are comparable in intensity, the explicit identification of the intra- and interresidue cross peaks can then be obtained by comparing the in-phase data set and two subspectra. The coherence transfer efficiency is usually much better for the residues in which the one- and two-bond couplings have similar size (*vide infra*). Thus, the loss of factor $\sqrt{2}$ in sensitivity for these residues, due to the identification between sequential and intraresidual connectivities by the spin-state-selection, is partly compensated by the inherently more efficient coherence transfer.

The coherence transfer efficiencies for the CT-HN(CO)CA and the proposed MP-CT-HNCA experiments were compared for the differing parts. For CT-HN(CO)CA transfer efficiency is given by Equation 2:

$$\sin^2(2\pi\,^1J_{NC'}T_N)\sin^2(2\pi\,^1J_{C'C^\alpha}T_C)$$
$$\exp(-4T_N/T_{2N})\exp(-4T_C/T_{2C'}), \qquad (2)$$

in which $^1J_{NC'}$ is 15 Hz, $^1J_{C'C^\alpha}$ is 53 Hz, $2T_N \sim$ 33 ms, $2T_C \sim$ 9.1 ms. The coherence transfer efficiency calculated for the CT-HN(CO)CA experiment is presented in Figure 3c using values of 7 and 50 ms for $T_{2C'}$ and T_{2N}, respectively. The coherence transfer efficiency in this case is 0.041 (see Figure 3).

Analogously for the sequential correlation in the antiphase MP-CT-HNCA experiment, the coherence transfer efficiency is given by Equation 3:

$$\sin^2(2\pi\,^2J_{NC^\alpha}T_a)\cos^2(2\pi\,^1J_{NC^\alpha}T_a)$$
$$\sin(2\pi\,^1J_{NC'}T_b)\exp(-2(T_a+T_b)/T_{2N}), \qquad (3)$$

where $^2J_{NC^\alpha} \sim$ 5–9 Hz, $^1J_{NC^\alpha} \sim$ 7–12 Hz, $2T_b =$ 33 ms and $2T_a \sim$ 24–28 ms. Using nominal values of 7 and 10 Hz for $^2J_{NC^\alpha}$ and $^1J_{NC^\alpha}$, respectively, and 50 ms for T_{2N} yields a coherence transfer efficiency of 0.043 for the sequential correlation in the MP-CT-HNCA experiment. Sensitivity of the MP-CT-HNCA experiment is further suppressed by the $^1J_{C^\alpha C'}$ modulation if a long t_1 ($> 1/(2J_{C^\alpha C'})$) is used. Assuming

that one- and two-bond couplings have the same value, 9 Hz for instance, the coherence transfer efficiency is 0.076. Hence, the sensitivity loss due to the spin-state-selective filtering is less harmful for the sequential cross peaks with large two-bond couplings, that is, for the cross peaks where the spin-state-selection is crucial to distinguish between inter- and intraresidual connectivities due to their similar intensity. In addition, the spin-state-selective filter used in the ^{15}N-^{13}C$^\alpha$ out-transfer also decreases the sensitivity of the MP-CT-HNCA experiment compared to the HNCA experiment due to a ∼5–8 ms longer transfer period. On the other hand, as the CT-HNCA and the CT-HN(CO)CA experiments are run in pairs, whereas for the proposed approach only one experiment is needed, the sensitivity loss due to coupled evolution is partly compensated by the two times shorter overall experimental time required. In principle, the proposed experiment can be run as a real-time, instead of the constant-time, ^{13}C$^\alpha$-evolution experiment for improved sensitivity, although we have not tested this approach. In summary, the CT-HN(CO)CA experiment is on average more sensitive for small proteins than the MP-CT-HNCA experiment, which is preferred for very large proteins at the highest magnetic fields currently available. In addition, the coherence transfer efficiency in the HNCA-type experiments has significant dependence on sizes of one- and two-bond couplings between amide nitrogen and alpha carbons, and for this reason cross peak intensity varies from one residue to another.

The MP-CT-HNCA experiment was tested on the uniformly ^{15}N, ^{13}C and ^{2}H labeled 30.4 kDa protein E2, at 5 °C. Figure 4 represents F_1-F_3 planes from the overlaid MP-CT-HNCA-TROSY (a) and the HN(CO)CA-TROSY (b) spectra. The sequential cross peaks in the MP-CT-HNCA spectrum are more intense for some residues, in particular for the weakest correlations, and for the residues where $^1J_{NC^\alpha} \sim\,^2J_{NC^\alpha}$. However, the HN(CO)CA experiment shows higher or equal intensity for many interresidual connectivities. This is in good agreement with our estimate of $T_{2C'}$ for E2 in 5 °C at 800 MHz, obtained by varying the length of the in-phase ^{13}C'-^{13}C$^\alpha$ filter in the HNCO(α/β-C'C$^\alpha$-J)-TROSY experiment (Permi et al., 2000) and monitoring signal intensity in 1D mode. A value of ∼ 15 ms for $T_{2C'}$ implies that HN(CO)CA should be more sensitive than the proposed experiment.

Conclusions

A new experiment enabling sequential assignment without relaying magnetization through $^{13}C'$ has been presented. The proposed experiment is optimal for the proteins and protein complexes with a rotational correlation time beyond 35 ns at the highest magnetic fields where T_2 of the $^{13}C'$ spin can be less than 10 ms. The MP-CT-HNCA experiment can be used together with the HNCACB experiment to provide much the same information as available through the CT-HNCA and CT-HN(CO)CA experiments. The proposed method is expected to be most efficient for assigning very large proteins. It is also suitable for the assignment of proteins expressed with utilizing segmental isotope labeling techniques (Yamazaki et al., 1998; Otomo et al., 1999). On the other hand, the MP-CT-HNCA experiment can also be useful for studying complexes with molecular weight beyond 70–80 kDa, in which the labeled protein itself is relatively small, i.e., 15–30 kDa.

Acknowledgements

References

Andersson, P., Weigelt, J. and Otting, G. (1998a) *J. Biomol. NMR*, **12**, 435–441.

Andersson, P., Annila, A. and Otting, G. (1998b) *J. Magn. Reson.*, **133**, 364–367.

Astrof, N., Bracken, C., Cavanagh, J. and Palmer III, A.G. (1998) *J. Biomol. NMR*, **11**, 451–456.

Gardner, K.H. and Kay, L.E. (1998) *Annu. Rev. Biophys. Biomol. Struct.*, **27**, 357–406.

Grzesiek, S. and Bax, A. (1993) *J. Am. Chem. Soc.*, **115**, 12593–12594.

Hu, J.S. and Bax, A. (1997) *J. Am. Chem. Soc.*, **119**, 6360–6368.

Konrat, R., Yang, D. and Kay, L.E. (1999) *J. Biomol. NMR*, **15**, 309–313.

Loria, J.P., Rance, M. and Palmer III, A.G. (1999) *J. Magn. Reson.*, **141**, 180–184.

Marion, D., Ikura, M., Tschudin, R. and Bax, A. (1989) *J. Magn. Reson.*, **85**, 393–399.

Meissner, A., Duus, J.Ø. and Sørensen, O.W. (1997) *J. Biomol. NMR*, **10**, 89–94.

Meissner, A., Schulte-Herbrüggen, T. and Sørensen, O.W. (1998a) *J. Am. Chem. Soc.*, **120**, 3803–3804.

Meissner, A., Schulte-Herbrüggen, T., Briand, J. and Sørensen, O.W. (1998b) *Mol. Phys.*, **95**, 1137–1142.

Otomo, T., Teruya, K., Uegaki, K., Yamazaki, T. and Kyogoku, Y. (1999) *J. Biomol. NMR*, **14**, 105–114.

Ottiger, M., Delaglio, F. and Bax, A. (1998) *J. Magn. Reson.*, **131**, 373–378.

Permi, P. and Annila, A. (2000) *J. Biomol. NMR*, **16**, 221–227.

Permi, P., Sorsa, T., Kilpeläinen, I. and Annila, A. (1999a) *J. Magn. Reson.*, **141**, 44–51.

Permi, P., Heikkinen, S., Kilpeläinen, I. and Annila, A. (1999b) *J. Magn. Reson.*, **140**, 32–40.

Permi, P., Rosevear, P.R. and Annila, A. (2000) *J. Biomol. NMR*, **17**, 43–54.

Pervushin, K., Riek, R., Wider, G. and Wüthrich, K. (1997) *Proc. Natl. Acad. Sci. USA*, **94**, 12366–12371.

Pervushin, K.V., Wider, G. and Wüthrich, K. (1998) *J. Biomol. NMR*, **12**, 345–348.

Rance, M., Loria, P. and Palmer III, A.G. (1999) *J. Magn. Reson.*, **136**, 92–101.

Salzmann, M., Pervushin, K., Wider, G., Senn, H. and Wüthrich, K. (2000) *J. Am. Chem. Soc.*, **122**, 7543–7548.

Shaka, A.J., Keeler, J., Frenkiel, T. and Freeman, R. (1983) *J. Magn. Reson.*, **52**, 335–338.

Shan, X., Gardner, K.H., Muhandiram, D.R., Rao, N.S., Arrowsmith, C.H. and Kay, L.E. (1996) *J. Am. Chem. Soc.*, **118**, 6570–6579.

Spezio, M., Wilson, D.B. and Karplus, P.A. (1993) *Biochemistry*, **32**, 9906–9916.

Szyperski, T., Braun, D., Fernandez, C., Bartels, C. and Wüthrich, K. (1995) *J. Magn. Reson.*, **108**, 197–203.

Weigelt, J. (1998) *J. Am. Chem. Soc.*, **120**, 10778–10779.

Yamazaki, T., Lee, W., Revington, M., Mattiello, D.L., Dahlquist, F.W., Arrowsmith, C.H. and Kay, L.E. (1994) *J. Am. Chem. Soc.*, **116**, 6464–6465.

Yamazaki, T., Lee, W., Arrowsmith, C.H., Muhandiram, D.R. and Kay, L.E. (1994) *J. Am. Chem. Soc.*, **116**, 11655–11666.

Yamazaki, T., Otomo, T., Oda, N., Kyogoku, Y., Uegaki, K., Ito, N., Ishino, Y. and Nakamura, H. (1998) *J. Am. Chem. Soc.*, **120**, 5591–5592.

Yang, D. and Kay, L.E. (1999) *J. Biomol. NMR*, **13**, 3–9.